Integrated Scramjet Installation Effect on the Subsonic Performance of a Hypersonic Aircraft

P. J. Johnston,* J. L. Pittman,† and J. K. Huffman‡
NASA Langley Research Center, Hampton, Va.

Various factors contributing to the high drag caused by the installation of a six-module scramjet engine were determined from wind-tunnel tests at Mach numbers from 0.2 to 0.7. Methods for alleviating this drag were also explored. The external exhaust nozzle, required for good cruise performance, was a major contributor. Of the drag produced by the engine modules, a significant fraction was attributable to wall divergence in the combustor. Good drag simulation could be achieved by using a single fuel injection strut having approximately the same cross-sectional area as the three used on the full-scale engine. External exhaust nozzle fences had a small but beneficial effect on maximum L/D, and a flap that diverted the flow away from the inlet was effective in decreasing drag but only at low angles of attack.

Nomenclature

C_A = axial force coefficient = axial force/qS
C_D = drag coefficient = drag/qS
C_L = lift coefficient = lift/qS
C_m = pitching moment coefficient = moment/qSl, about $0.65l$
C_p = pressure coefficient
L/D = lift-drag ratio
l = body length = 5.75 ft
M = Mach number
q = dynamic pressure
Re = Reynolds number
S = planform area of wing = 6.05984 ft^2
α = angle of attack, deg

Subscripts

max = maximum
min = minimum
eng = engine

Introduction

IN 1974-1975, joint U.S. Air Force/NASA studies of an advanced hypersonic research airplane indicated the feasibility of designing a vehicle capable of sustained cruise flight at Mach numbers up to 6 utilizing scramjet propulsion.[1,2] Although a number of candidate configurations were examined in these studies, a feature common to each was the bottom-mounted, fixed-geometry, modular scramjet engine. For this type of installation, the entire vehicle lower surface serves as part of the propulsion system, with the forebody providing precompression of the air and the afterbody serving as the exhaust nozzle. The importance of the external nozzle to engine performance is exemplified by the fact that it provides about half of the engine net thrust at Mach 6.

Subsequent to the studies, wind-tunnel models were constructed for tests over the speed range from Mach 0.2 to 6.0 to validate theoretical predictions of stability, performance, and aerodynamic heating. To accomodate entry into several wind tunnels, the stability and performance models were chosen to be approximately 1/30 scale and were constructed so that a simulated scramjet could be installed to represent the aircraft in those segments of the flight profile where the engine was unlit, e.g., rocket ascent, rocket cruise with unlit scramjet, and unpowered descent and landing.

The small size of these models made it impractical to duplicate all of the internal geometry of the full-scale engine. (At 1/30 scale, the inlet height was only 0.6 in., and fuel injection struts, for example, would have had maximum thickness of only about 1/32 in.) Instead, only the exterior lines and module sidewall partitions were modeled. In addition, a single large strut was used to simulate the combined blockage of the three fuel injection struts required in each module of the full-scale engine design. Finally, in the rear or combustor section of the engine, the upper walls did not incorporate the internal geometry representative of the flight engine.

Results from these tests showed that the scramjet installation caused a substantial loss in performance over the entire Mach number range, but these penalties were of particular concern at low speeds because of the desire to achieve a landing L/D in excess of 3.0. Reference 3 indicated that this L/D was about the minimum acceptable for safe dead-stick landings.

Beyond the immediate concern of the research aircraft mission, however, the subsonic-transonic drag of the scramjet

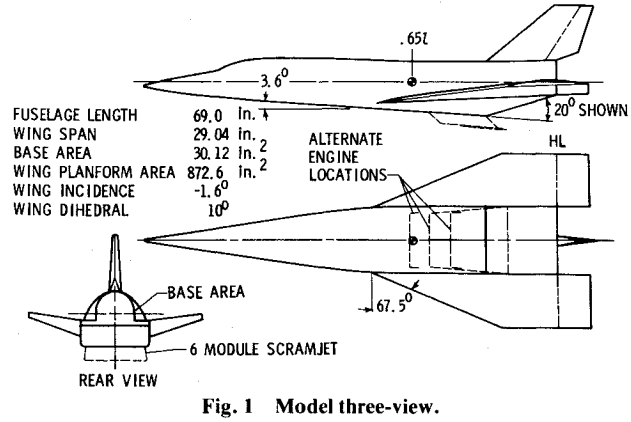

Fig. 1 Model three-view.

Presented as Paper 77-1230 at the AIAA Aircraft Systems and Technology Meeting, Seattle, Wash., Aug. 22-24, 1977; submitted Sept. 1, 1977; revision received March 9, 1978.

Index categories: Aerodynamics; Transonic Flow; Airbreathing Propulsion

*Aero-Space Technologist, Hypersonic Aerodynamics Branch, HSAD. Member AIAA.

†Aero-Space Technologist, Hypersonic Aerodynamics Branch, HSAD.

‡Aero-Space Technologist, Fluid Dynamics Branch, STAD.

installation could have a significant implication for future hypersonic vehicles such as transports, first-stage air-breathing launch vehicles, etc. As currently envisioned, many of these systems would takeoff and accelerate on turbojet power and convert to dual-mode scramjet propulsion in the neighborhood of Mach 3. Details of the installation of the combined engine system are not yet clear, but it is intuitively evident that oversizing the turbomachinery to overcome the scramjet drag would penalize overall mission performance significantly in terms of range and payload.

This paper summarizes the highlights of the study of the scramjet installation drag on a research airplane configuration at subsonic speeds. The 1/10-scale model was large enough to allow a near exact duplication of the engine interior geometry and also permit the installation of numerous static pressure orifices ahead of, inside, and downstream of the engine. Results, particularly from integration of these engine pressure distributions, permitted the important sources of installation drag to be sorted out and assessed. The forces produced by the various components should be applicable in installation studies of similar scramjet-powered aircraft with appropriate corrections for the ratio of inlet to reference area.

Experiments

Model and Instrumentation

Airframe

A sketch of the wind-tunnel is shown in Fig. 1. The configuration was attached to a six-component internal strain gage balance, which was sting-supported. Fuselage base pressures were measured and the force data adjusted to a condition where freestream pressure acted over the base.

To detect the upstream influence of the engine, 10 static pressure orifices were arrayed on the left-hand side of the fuselage lower surface ahead of the engine. Up to 36 orifices were also installed on the left-hand side of the external nozzle in order to determine the force and moment contributions of this component. Exhaust nozzle angles of 16, 20, and 24 deg were obtained by varying the longitudinal position of the scramjet engine while holding the nozzle-base intersection fixed.

Engine

An oblique view of the scramjet modules is shown in Fig. 2. The complete engine model consisted of six modules located symmetrically with respect to the vehicle plane of symmetry. For better alignment with the forebody flow at hypersonic speeds, the centerline of each module was diverged 1 deg from adjacent modules in the streamwise direction. The three left-hand modules, designated inboard, middle, and outboard, were instrumented with 12 orifices each, as illustrated in Fig. 3. The shallow diamond cross section of the module sidewall partition prevented pressure tubing from being installed near the leading edge, and so the first three orifices in each inlet were located in the top wall of the engine on a 1.2-in. spacing beginning at the inlet station.

One of the important aspects of this study was to determine the degree of internal geometric simulation necessary for correct engine drag representation; hence several modifications were made to the engine interior geometry. These include 1) the removal of the combustor block from each module, 2) replacement of the three simulated fuel injection struts by a single large strut of approximately the same blockage, and 3) for reference, the removal of all struts. Details of the three simulated fuel injection struts are given in Fig. 4, along with the geometry of the single large strut. Also shown here and in Fig. 3 is the sidewall area relief found to be required to alleviate a local blockage problem.[4]

In addition to the foregoing internal changes, several exterior modifications were examined, including the deployment of a 15-deg ramp on the forebody ahead of the inlet. The height of the ramp was equal to the inlet height, and its width

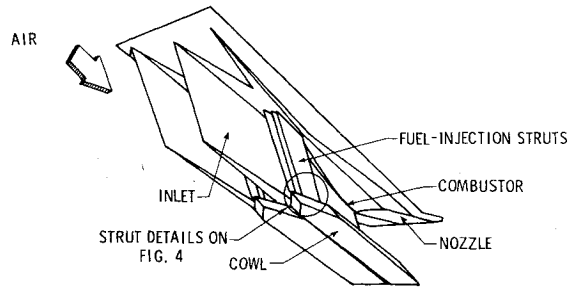

Fig. 2 Oblique view of scramjet modules.

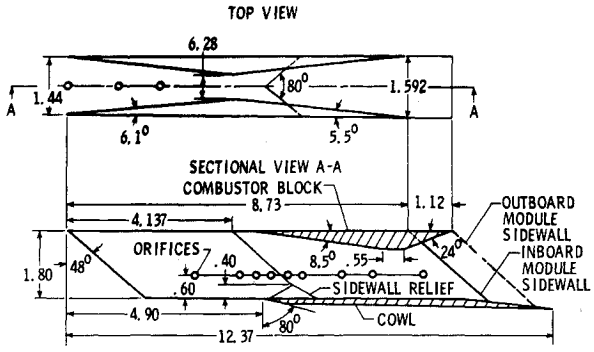

Fig. 3 One-tenth scale scramjet module geometry.

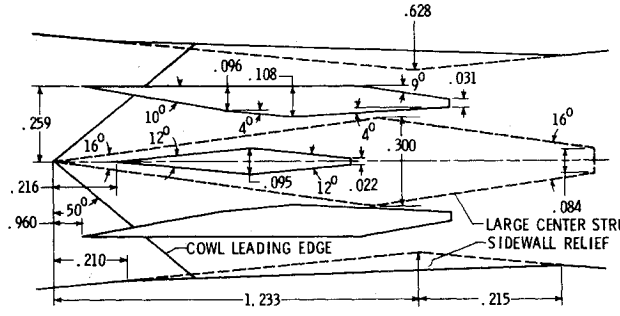

Fig. 4 Strut details in vicinity of module throat-cowl intersection.

was about 5% greater than the total inlet width of 8.64 in. The ramp base was instrumented for pressures and was located 0.4 in. ahead of the inlet.

Exhaust nozzle fences, which might offer some beneficial performance effects at hypersonic speeds, were also tested in conjunction with the 24-deg nozzle. The fences were simple rectangular planform (1.625 × 13 in.) plates attached normal to the nozzle surface and diverged at the same 3-deg angle as the outboard engine sidewalls.

Wind Tunnel and Tests

The tests were conducted in the Langley 7- × 10-ft wind tunnel at atmospheric stagnation pressures. Reynolds numbers based on fuselage length varied with Mach number as follows: $M=0.2$ and $Re=7.5\times10^6$; $M=0.4$ and $Re=14.1\times10^6$; $M=0.6$ and $Re=19.0\times10^6$; and $M=0.7$ and $Re=21.0\times10^6$. By the way of comparison, the full-scale vehicle would have Reynolds numbers of the order of 100×10^6 at comparable speeds.

For this type of engine installation, which is designed to swallow the forebody boundary layer, it was considered important that the full-scale boundary-layer conditions be simulated as closely as possible. Thus, transition strips consisting of ⅛-in.-wide No. 120 carborundum particles were used to trip the boundary layer, following the recommendations of Ref. 5. Trips were applied at 5% of the local

streamwise length on all airframe and engine aerodynamic surfaces except the simulated fuel injection struts and cowl interior surface. This grit size provided a critical roughness Reynolds number of 600 at Mach 0.4 but, of course, was somewhat larger than necessary at the higher Mach numbers because of increasing unit Reynolds number. However, as noted in Ref. 5, this situation would not produce measurable roughness drag.

There was some concern regarding the effectiveness of the roughness elements at $M=0.2$ because of the low Reynolds numbers at the trip locations. Boundary-layer stability theory[6] predicts that a two-dimensional laminar boundary layer has sufficient stability to damp out small disturbances at displacement thickness Reynolds numbers below 420. Calculations showed, however, that the laminar displacement thickness Reynolds numbers at the trip locations exceeded this critical value on all aerodynamic surfaces except the engine cowl exterior and module partitions. On these surfaces, it was about 20% low, and ostensibly, therefore, the boundary layers could not be tripped at $M=0.2$. About 40% of the partition height was immersed in the turbulent fuselage boundary layer, which, in conjunction with the partition roughness elements, may have been adequate to encourage early transition.[7] The flow on the cowl exterior surface was somewhat unique in that unpublished oil flow studies indicated that it was highly complex and dominated by vortices produced by the impingement of spillage flows from the individual modules interacting with the sharp, saw-tooth leading edges. Whether the criterion of laminar stability theory can be applied rigidly in this complex flow situation is doubtful, and more definitive tests would be required to ascertain the state of the boundary layer on the cowl surface and the efficacy of transition strips.

Data Reduction

Balance and pressure data were reduced to coefficients in the usual manner. The bookkeeping method of obtaining the contribution of the six-module engine was as follows. For axial force,

$$C_{A_{\text{engine}}} = (C_{A_{\text{balance}}} - C_{A_{\text{nozzle}}})_{\text{engine installed}} - (C_{A_{\text{balance}}} - C_{A_{\text{footprint}}} - C_{A_{\text{nozzle}}})_{\text{clean}}$$

Nozzle forces were obtained by integration of pressure distributions. The engine footprint force was determined as follows: pressures on the forebody were integrated to obtain a spanwise average on the clean configuration, and these average pressures were assumed to persist rearward over the footprint of the engine. In the axial direction, the forces were very small (0.0015 maximum) because of the shallow slope of the forebody. The engine module forces resulting from the foregoing equation are installed values that include mutual interference effects between the engine and airframe, spillage, friction, vorticity, etc.

Two interior engine forces, designated inlet and combustor, were obtained from integration of the module sidewall pressure distributions. Inlet forces were conveniently separated from combustor forces by integrating downstream to the swept ridge line, which is the maximum thickness location of partitions (cf. Fig. 3). Axial forces were resolved by taking into account local surface slopes, including the fact that the partitions were diverged 1 deg from each other.

The greatest potential source of error for these interior engine forces was the assumption that the pressures were constant in the vertical plane. Despite this uncertainty, it is believed that the results provide a good quantative measure of the relative magnitude of the forces in the engine inlet and combustor and from one module to another.

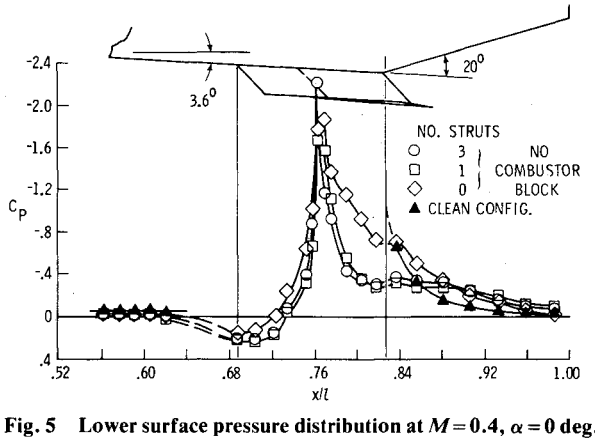

Fig. 5 Lower surface pressure distribution at $M=0.4$, $\alpha=0$ deg.

Results and Discussion

Engine Internal Geometry

Pressure Distributions

To aid in visualizing the character of the flow in the vicinity of the engine, typical pressure distributions at $M=0.4$ and $\alpha=0$ deg are shown in Fig. 5 for the tests involving removal of the fuel struts. Pressure coefficients are shown along the fuselage centerline ahead of the inlet, through the inboard module, and on the external nozzle along a row of orifices coinciding with an extension of the module centerline. The solid symbols are pressure coefficients on the clean aircraft.

Although the differences in pressure coefficient are small, Fig. 5 shows that the upstream influence of the engine extends beyond the first orifice, which, for this engine position, was 4.78 inlet heights ahead of the engine; because of the limited number of forebody orifices, however, this pre-entry drag could not be accurately resolved. Compared to other engine components, its contributions to axial force is small because of the shallow forebody angle; but, because of the large areas involved, it may have a significant effect on the normal force component.

As the flow proceeds toward the engine, the pressure coefficients begin to rise more rapidly, reaching a maximum just inside the inlet. Thereafter, the internal flow undergoes a rapid acceleration to the module throat and decelerates in the combustor and over the external nozzle.

Comparison of the one- and three-strut data shows relatively good agreement in both the inlet and combustor. Pressure coefficients for the configuration without fuel struts, however, are somewhat more negative throughout the inlet but, more importantly, are substantially more negative downstream in the engine combustor section and over the initial 40% of the external nozzle. Both the combustor sidewalls and the nozzle surface have downstream facing slopes, of course, and the occurrence of these low-pressure regions are factors that contribute to higher installation axial force of the configuration without fuel struts. The full impact of these low pressures is not realized however, because without the fuel struts, more negative pressure coefficients occur in the inlet section which partially compensate for the larger combustor axial force.

Effect of Inlet Struts

Pressure distributions such as those just discussed were integrated to determine the magnitude of the drag contribution of the individual engine components; typical results are shown in Fig. 6. In this mode of presentation, the difference between the total engine force and the combustor force is designated "interaction" but is actually a combination of several factors, such as inlet spillage, mutual interference between the engine and airframe, engine skin friction, pre-entry drag, vorticity produced by the sharp edges of the engine exterior surfaces, and by the saw-tooth cowl leading edge. In Fig. 6, the total installation drag can be

determined by subtracting the appropriate inlet force component from the maximum values shown.

Two important features are evident in the figure: 1) the substitution of a single large strut of equivalent blockage provided an excellent simulation of the drag of the three struts required in each module of the actual engine; and 2) the removal of all struts caused significant changes in the drag of various components but, because of compensating effects, the total installation drag was not significantly affected. One beneficial implication of these results is that considerable cost savings should accrue in future wind-tunnel model construction of scramjet-powered aircraft equipped with this type of engine, since only one-third of the actual number of struts need be fabricated. Removal of the struts not only caused relatively large changes in the inlet and "interaction" (i.e., spillage) forces that were anticipated, but also had a considerable impact on the drag of components farther downstream, that is, the combustor and external nozzle.

To provide a basis for judging the size of the installation forces and to provide further emphasis of their magnitude relative to the airframe forces, the value of minimum drag coefficient of the clean aircraft and the calculated engine turbulent skin friction have been identified on the ordinate of Fig. 6. It may be noted, for example, that without the struts the drag of the combustor section alone is nearly equal to that of the entire airframe in the clean configuration.

Figure 7 shows the strut effect on the overall airframe stability and performance. The one- and three-strut data are in excellent agreement in lift, drag, and pitching moment at both Mach numbers. Without the struts, however, the drag at Mach 0.4 was in good agreement, but at Mach 0.6 it was uniformly high; this may be an indication that the configuration without the struts will be more sensitive to Mach number in the transonic regime. At low and moderate angles of attack, the configuration without struts had consistently smaller lift coefficients, which may be attributable both to the different spillage characteristics when the struts are removed and to lower pressures on the external nozzle. Pitching moments without the struts were more negative at high angles of attack than for either the one- or three-strut configurations; apparently this is related to different spillage characteristics, since the more negative pressure coefficients occurring on the nozzle when the struts were removed would have caused the opposite effect on C_m.

In summary, then, the single large strut was shown to be an excellent means of simulating the effects of the three struts on both engine interior and overall vehicle forces and moments. Removal of the struts, however, produced significant changes in the engine interior forces coupled with a larger exhaust nozzle drag contribution. In addition, the aircraft had less lift and generally more negative pitching moments without the struts and, for all of these reasons, is considered an unsatisfactory method of simulation.

Spanwise Variation in Module Forces

A problem unique to the modular engine design considered here is the effect of forebody flow and module divergence on engine forces. A module divergence of 1 deg was a compromise based on the hypersonic forebody design analysis of Ref. 8. Streamline divergence, on the other hand, is an intrinsic characteristic of windward flows on bodies and varies with angle of attack. Inasmuch as this divergence was not measured in the investigation, its effects could only be inferred from the differences in the spanwise distribution of module forces over a wide angle-of-attack range.

Figure 8 shows the distribution of engine interior forces at angles of attack of 0 and 20 deg, and the close similarity in these distributions suggests that module divergence was more important than flow divergence in determining either the inlet or combustor axial forces. Furthermore, these results infer that exact number of modules of the full-scale engine should

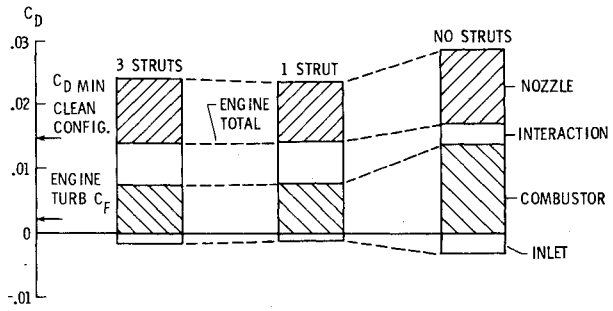

Fig. 6 Effect of struts on engine component drag ($M=0.4$, $\alpha=0$ deg), no combustor block.

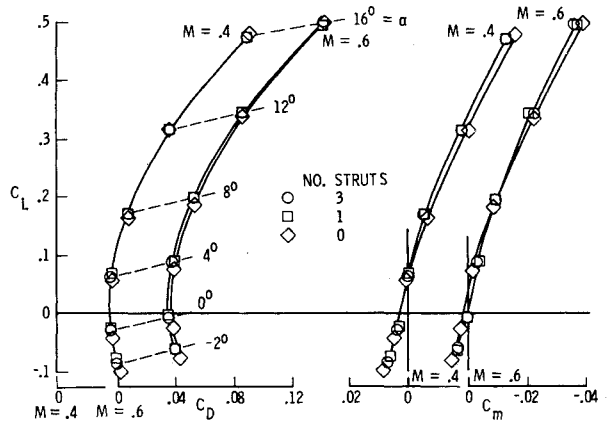

Fig. 7 Effect of struts on total vehicle stability and performance.

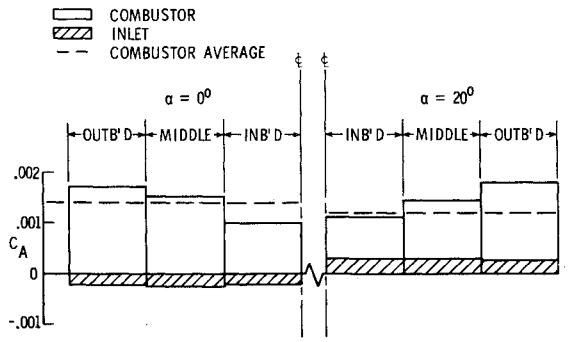

Fig. 8 Spanwise variation of engine force components ($M=0.4$), three struts, standard combustor.

be duplicated in subscale tests; i.e., forces on a three-module engine, even if nondimensionalized by inlet area, would not be representative of the corresponding forces on a six-module engine. In preliminary design work, it may be necessary to use an average value for one of these interior forces in lieu of an actual spawise distribution; the effect of this assumption on the combustor section force is illustrated in Fig. 8.

Combustor Geometry

Figure 9 indicates that changing the upper wall contour in the combustor section of the engine had little effect on the overall vehicle aerodynamic characteristics. An examination of the engine interior force components showed that the small changes that did occur were confined primarily to the engine rather than spreading downstream to the external nozzle, as was the situtation when the inlet struts were removed. It should not be implied from these limited results that duplication of combustor geometry is of secondary importance for good aerodynamic simulation, because, as will

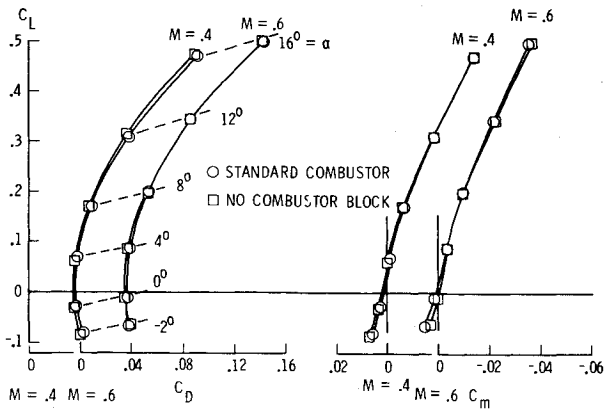

Fig. 9 Effect of combustor geometry on longitudinal characteristics, three struts, 20-deg nozzle.

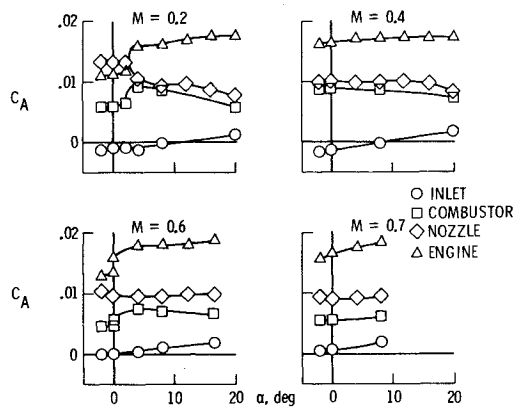

Fig. 11 Engine component axial forces, three struts, standard combustor, 20-deg nozzle.

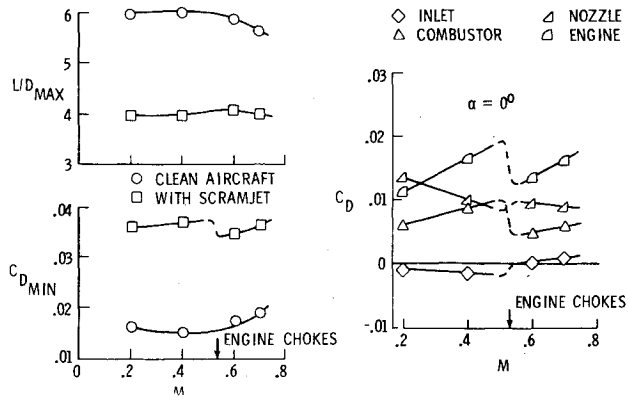

Fig. 10 Effect of Mach number on vehicle performance and engine drag components, three struts, standard combustor, 20-deg nozzle.

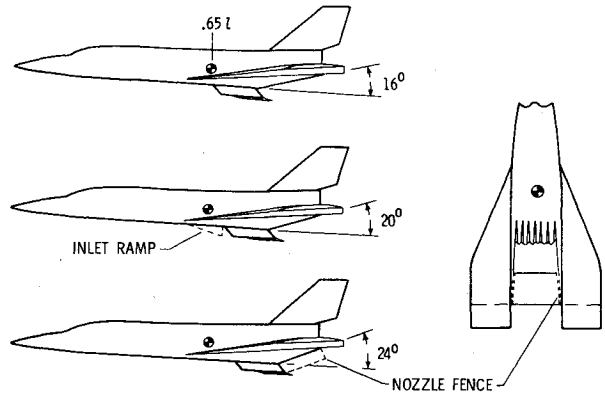

Fig. 12 External geometry modifications.

be shown later, flow changes occurring in this segment of the engine had important effects on vehicle characteristics both at low speeds and near the choking Mach number.

Mach Number Effects

Although the previous results emphasized the effects of alterations in the engine internal geometry on forces and moments, Fig. 10 shows the effect of Mach number on vehicle performance and engine force characteristics. Shown on the left of this figure are minimum drag coefficient and L/D_{max} of the configuration with and without the engine. Perhaps the outstanding feature illustrated here is that the engine installation more than doubled the minimum drag of this particular configuration. Furthermore, with the engine installed, there was an apparent abrupt decrease in $C_{D_{min}}$ Near the Mach number at which the engine chokes, but this rapid decrease in drag did not persist at higher angles of attack. Examination of both lift and drag forces at the angles of attack for L/D_{max} showed gradual variations with Mach number which, of course, resulted in the smooth trend of L/D_{max} with Mach number shown in the figure.

The engine components contributing to the abrupt variations in vehicle drag are illustrated on the right of Fig. 10. It is evident that the dominant factor was a change in flow pattern in the combustor at the choking Mach number, resulting in the precipitous drop in total engine drag. Below the choking Mach number, the combustor section produces about half of the engine drag, but this fraction decreases at higher speeds because spillage forces increase (as reflected by the larger inlet force), and the internal mass flow ratio has reached its maximum value at the choking speed.

The external nozzle produced the largest contribution to drag at low speeds, but its magnitude decreased through the speed range except for the interval near the choking speed. As noted in the discussion on the effect of fuel struts, a compensating effect occurs between the engine components, with the nozzle drag reduction tending to offset the increased drag of the engine.

Figure 11 shows that, in addition to Mach number, angle of attack also caused abrupt changes in the installation forces. At Mach 0.2, for example, there were abrupt increases in both combustor and total engine axial forces at $\alpha \approx 3$ deg which were accompanied by a reduction in the external nozzle force. A similar increase in combustor and total engine forces occurred again at Mach 0.6, but, in contrast to the low-speed results, these increases were not accompanied by the compensating decreases in nozzle force, which suggests the occurrence of a different flow mechanism once supersonic flow was established either inside or exterior to the engine.

External Geometry Variations

The external geometry modifications examined during the investigation are illustrated in Fig. 12; these include deflecting a flap or ramp ahead of the inlet, the addition of fences to the 24-deg nozzle, and varying the engine longitudinal position on the body. The intent of the latter was to provide parametric data as a basis for tradeoffs between reduced hypersonic power-on trim drag penalties (from the proper selection of engine location[9]) and subsonic performance benefits resulting from decreased nozzle drag.

Inlet Ramp

Although originally conceived as a means of reducing spillage effects, the inlet ramp may have other highly practical uses, such as protecting the engine from a hot environment during descent or in the event coolant flow is interrupted. Another possible application for the research airplane mission is to protect the numerous sharp leading edges of the engine

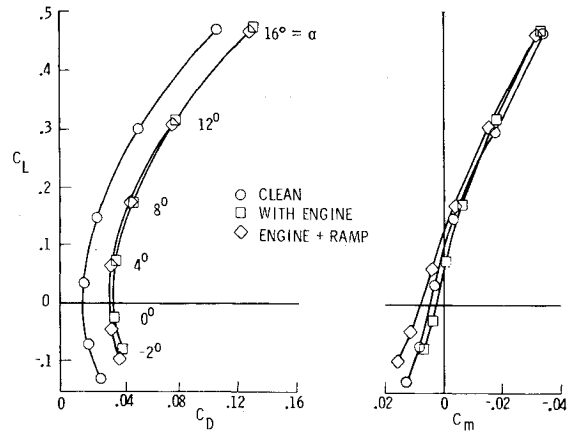

Fig. 13 Effect of inlet ramp on pitch characteristics at $M=0.4$, three struts, standard combustor.

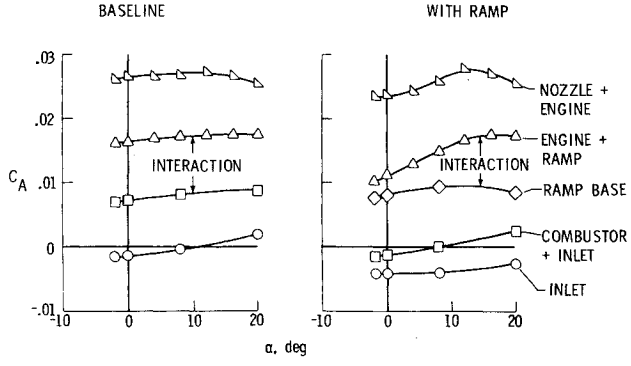

Fig. 14 Effect of inlet ramp on installation forces at $M=0.4$, three struts, standard combustor, 20-deg nozzle.

from ground debris thrown up by the nose landing gear, especially during possible emergency landings on unprepared lake beds. This use might be particularly important, since the clearance between the engine and ground is only a few inches for the configuration tested.

The drag polars in Fig. 13 show that the inlet ramp reduced minimum drag somewhat but did not improve L/D_{max}. In addition, the ramp caused a reduction in lift and increased the nose-up pitching moment throughout the angle-of-attack range. Moment coefficients with and without the ramp bracketed those of the clean configuration at low angles of attack.

Figure 14 indicates why the drag reductions produced by the ramp were not sustained over the angle-of-attack range. As expected, the ramp decreased the engine internal forces (inlet and combustor), but, in addition, it produced a large drag contribution because of suction pressures acting over its base. The ramp effectively reduced the "interaction" term (i.e., spillage) at low angles of attack; however, this axial force component increased rapidly with angle of attack, suggesting that the flow spilled off the ramp and entered the engine, with the result that the combined ramp and engine axial force had about the same magnitude as the baseline engine configuration at angles of attack near L/D_{max}. It may also be noted that, by deflecting the flow away from the engine at low angles of attack, the ramp caused the external nozzle axial force contribution to be somewhat greater than that for the baseline engine installation.

Conceivably, a more sophisticated ramp geometry could be devised which would have prevented flow from entering the engine, thus maintaining the "interaction" term at the level measured at $\alpha=0$ deg. Calculations show, however, that the L/D_{max} of the present configuration would have increased by only 0.2, and this small benefit would have to be weighed

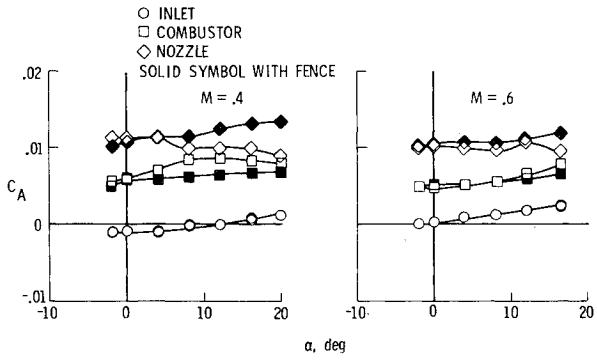

Fig. 15 Effect of nozzle fences on engine axial forces, three struts, standard combustor, 24-deg nozzle.

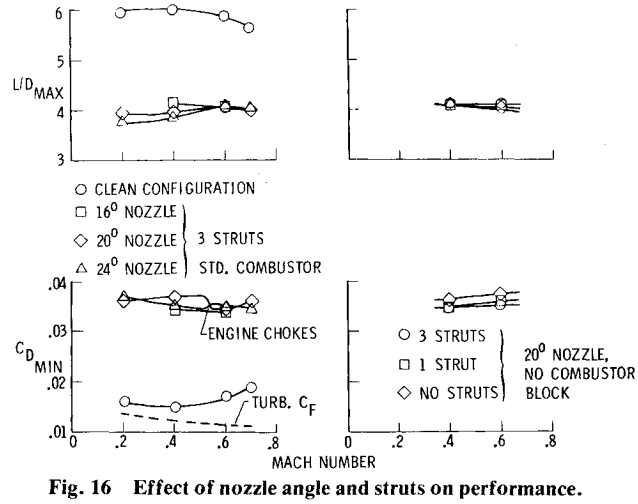

Fig. 16 Effect of nozzle angle and struts on performance.

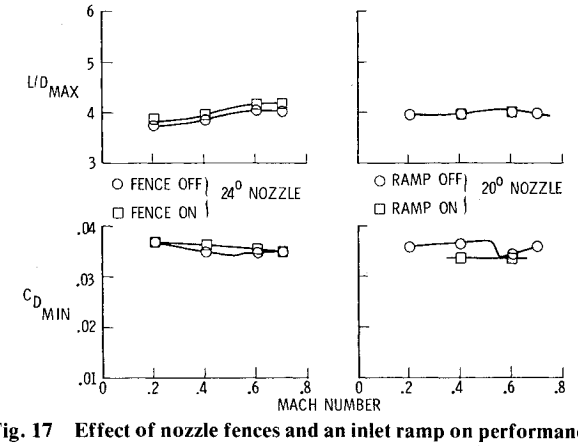

Fig. 17 Effect of nozzle fences and an inlet ramp on performance.

against the additional complexity of a ramp with "fingers" extending into the inlet of each module.

Nozzle Fences

It has been postulated that fences could improve hypersonic performance by 1) confining the engine exhaust to a nearly two-dimensional expansion, 2) eliminating potentially adverse interactions between the elevons and the adjacent exhaust flow, and 3) increasing the vehicle side area aft of its center of gravity in a region of relatively high q, thereby improving directional stability. These potential benefits, of course, must be weighed against the possibility of increased drag at lower speeds.

Figure 15 illustrates the effect of the fences on the installation axial forces at Mach numbers below and above the

engine choking speed. At $M=0.4$, the fences increased the nozzle axial force at moderate and high angles of attack, but this was offset by a reduction in combustor force because of the elimination of the asperating effect of the exterior flow at the engine sidewall trailing edge. Above the choking Mach number, the effect of the fences on the nozzle and combustor forces was substantially reduced over the angle-of-attack range, apparently because of the combination of choking the internal flow and the occurrence of local zones of supersonic flow outside the engine.

Concluding Remarks

An investigation has been made at subsonic speeds to determine the factors contributing to the high levels of drag produced by an unlit, highly integrated, six-module scramjet engine. An important issue addressed in these studies was the degree of geometric duplication necessary to provide good simulation of the actual engine forces and moments.

The results indicate that a single large inlet strut having approximately the same blockage as the three fuel injection struts used on the full-scale engine provided a good simulation of the flow in the inlet, combustor, and external exhaust nozzle. Complete removal of the struts produced large but mutually compensating changes in the engine and nozzle axial force components. In addition, the configuration had less lift and more negative pitching moments, which were attributable to the different inlet spillage characteristics without the struts.

Module divergence was shown to be an important factor that must be duplicated for accurate simulations. The entire engine installation should be tested as a unit because of the mutual interaction between the various components such as the combustor and external nozzle. Choking of the inlet flow or the possible existence of zones of supersonic flow outside the engine had a significant effect on the installation force components and consequently on overall vehicle drag.

A flap or ramp ahead of the engine inlet decreased minimum drag somewhat but was not effective at the angle of attack of L/D_{max} because of flow spilling off the ramp and entering the engine. Exhaust nozzle fences afforded limited improvements in vehicle performance despite the fact that they were diverged a total of 6 deg and increased the vehicle wetted area. Further investigation of fences may be warranted if their postulated hypersonic performance benefits are realized.

References

[1] Hearth, D. P. and Preyss, A. E., "Hypersonic Technology – Approach to an Expanded Program," *Astronautics and Aeronautics*, Vol. 14, Dec. 1976, pp. 20-37.

[2] Kirkham, F. S., Jones, R. A., Buck, M. L., and Zima, W. P., "Joint USAF/NASA Hypersonic Research Aircraft Study," AIAA Paper 75-1039, Aug. 1975.

[3] "Flight Test Results Pertaining to the Space Shuttlecraft," NASA TM X-2101, June 30, 1970.

[4] Trexler, C. A. and Souders, S. W., "Design and Performance at a Local Mach Number of 6 of an Inlet for an Integrated Scramjet Concept," NASA TN D-7944, Aug. 1975.

[5] Braslow, A. L. and Knox, C. E., "Simplified Method for Determination of Critical Height of Distributed Roughness Particles for Boundary Layer Transition at Mach Numbers from 0 to 5," NACA TN 4363, Sept. 1958.

[6] Schlichting, *Boundary Layer Theory*, McGraw-Hill, New York, 1955.

[7] Braslow, A. L., "A Review of Factors Affecting Boundary-Layer Transition," NASA TN D-3384, Aug. 1966.

[8] Edwards, C. L. W., "A Forebody Design Technique for Highly Integrated Bottom-Mounted Scramjets with Application to a Hypersonic Research Airplane," NASA TN-D-8369, Dec. 1976.

[9] Weidner, J. P., Small, W. J., and Penland, J. A., "Scramjet Integration on Hypersonic Research Airplane Concepts," *Journal of Aircraft*, Vol. 14, May 1977, pp. 460-466.